In Vivo Imaging of β-Cell Mass in Rats Using ^{18}F-FP-(+)-DTBZ: A Potential PET Ligand for Studying Diabetes Mellitus

Mei-Ping Kung[1], Catherine Hou[1], Brian P. Lieberman[1], Shunichi Oya[1], Datta E. Ponde[1], Eric Blankemeyer[1], Daniel Skovronsky[2], Michael R. Kilbourn[3], and Hank F. Kung[1,4]

[1]Department of Radiology, University of Pennsylvania, Philadelphia, Pennsylvania; [2]Avid Radiopharmaceuticals, Inc., Philadelphia, Pennsylvania; [3]Department of Radiology, University of Michigan, Ann Arbor, Michigan; and [4]Department of Pharmacology, University of Pennsylvania, Philadelphia, Pennsylvania

Recent studies on gene expression of β-cell mass (BCM) in the pancreas showed that vesicular monoamine transporter 2 (VMAT2) is highly expressed in the BCM (mainly in the islets of Langerhans). Imaging pancreatic BCM may provide an important tool for understanding the relationship between loss of insulin-secreting β-cells and onset of diabetes mellitus. In this article, 9-fluoropropyl-(+)-dihydrotetrabenazine (FP-(+)-DTBZ), which is a VMAT2 imaging agent, was evaluated as a PET agent for estimating BCM in vivo. **Methods:** Organ biodistribution after an intravenous injection of ^{18}F-FP-(+)-DTBZ (active isomer) and ^{18}F-FP-(−)-DTBZ (inactive isomer) was evaluated in normal rats. The specificity of uptake of ^{18}F-FP-(+)-DTBZ was assessed by a pretreatment (3.8 mg of (+)-DTBZ per kilogram and 3.5 mg of FP-(+)-DTBZ per kilogram, intravenously, 5 min prior) or coadministration (2 mg of (+)-DTBZ per kilogram). PET studies were performed in normal rats. **Results:** The in vivo biodistribution of ^{18}F-FP-(+)-DTBZ in rats showed the highest uptake in the pancreas (5% dose/g at 30 min after injection), whereas ^{18}F-FP-(−)-DTBZ showed a very low pancreas uptake. Rats pretreated with FP-(+)-DTBZ displayed a 78% blockade of pancreas uptake. PET studies in normal rats demonstrated an avid pancreas uptake of ^{18}F-FP-(+)-DTBZ. **Conclusion:** The preliminary data obtained with ^{18}F-FP-(+)-DTBZ suggest that this fluorinated derivative of DTBZ shows good pancreas specificity and has the potential to be useful for quantitative measurement of VMAT2 binding sites reflecting BCM in the pancreas.

Key Words: diabetes; beta-cell mass; pancreas imaging; VMAT2

J Nucl Med 2008; 49:1171–1176
DOI: 10.2967/jnumed.108.051680

The pancreas comprises 2 tissue types: exocrine and endocrine. The endocrine tissue accounts for only a small percentage of the pancreatic mass, is found scattered in the islets of Langerhans, and comprises predominantly β-cells. β-cells produce insulin in response to metabolic demands, and loss of β-cells results in insulin deficiency and diabetes. In type 1 diabetes, common in juveniles, an autoimmune process dramatically destroys β-cells. In type 2 diabetes, β-cell mass (BCM) decreases as part of a slower, more insidious process that also involves peripheral insulin resistance and increased demand for insulin. Because of a significant BCM reserve, symptoms related to unstable glucose homeostasis do not result until BCM is reduced by more than 50%–60% (*1*). Unfortunately, most studies measuring BCM have relied on postmortem examination of the pancreas, and until recently (*2,3*), it has been impossible to prospectively measure BCM in vivo.

Although no cure for diabetes exists, several promising potential therapies for modifying the disease course are in clinical trials. These approaches focus mainly on preserving or replacing BCM and include pancreas or islet cell transplantation (*4–8*) or islet cell regeneration from stem cells. The ability to monitor BCM in vivo will facilitate development of disease-modifying therapies for diabetes mellitus (*9–11*). Indeed, in the past few years many attempts have been made to image BCM; most of this work has been based on specific binding sites or receptors, such as sulfonylurea receptors and other binding sites in the pancreas (*12–15*). Studies using labeled β-cell–specific antibody and the fragment as in vivo imaging agents have shown some promise, but they are not suitable for routine clinical use because of a relatively low cellular specificity (low pancreas accumulation vs. high liver and kidney accumulations) (*16*). Additional BCM ligands have been reported, but except for the vesicular monoamine transporter 2 (VMAT2) imaging agents, none has been successfully applied to image diabetes in humans (*5–8,16–21*).

Recently, immunohistochemical staining studies of gene expression in the endocrine pancreas showed that VMAT2 binding sites are expressed mainly on the β-cells in the islets of Langerhans (*2,22*). VMAT2 expression matches

Received Feb. 11, 2008; revision accepted Apr. 3, 2008.
For correspondence or reprints contact: Hank F. Kung, Department of Radiology, University of Pennsylvania, 3700 Market St., Room 305, Philadelphia, PA 19104.
E-mail: kunghf@sunmac.spect.upenn.edu
COPYRIGHT © 2008 by the Society of Nuclear Medicine, Inc.

well with the insulin levels in human and monkey pancreas tissue (*23*). Therefore, VMAT2 could be an excellent target for mapping β-cell function. A VMAT2 ligand, (+)-^{11}C-dihydrotetrabenazine (DTBZ), was developed previously for imaging VMAT2 in the striatum. It has been successfully applied for PET studies of Parkinson's and other neurodegenerative diseases (*24,25*) and was recently used for PET VMAT2 binding sites in the pancreas of monkeys and humans (*1,2,26,27*). This is, to our knowledge, the first use of PET with (+)-^{11}C-DTBZ to measure the BCM in the pancreas, suggesting that PET of β-cells may be a useful tool to estimate the functional stage of these cells in living humans (*1*). It may also be possible to study the function of islet cells after transplantation (*28,29*). However, ^{11}C has a relatively short half-life ($t_{1/2}$ = 20 min), making clinical trials difficult and preventing longer imaging protocols that may be required to optimize imaging kinetics. In contrast, ^{18}F-labeled analogs of DTBZ, with a longer half-life ($t_{1/2}$ = 110 min), could be made more widely available through the same regional distribution network currently delivering ^{18}F-FDG to nuclear medicine clinics.

While developing ^{18}F-labeled analogs of DTBZ as imaging agents for Parkinson's disease, we have successfully tested a novel DTBZ derivative, an optically pure fluoropropyl derivative, ^{18}F-labeled 9-fluoropropyl-(+)-DTBZ (FP-(+)-DTBZ) (Fig. 1), in rodents and nonhuman primates (*30–32*). It displayed excellent binding affinity (K_i = 0.11 nM) for VMAT2. The higher binding affinity (lower K_i value) of FP-(+)-DTBZ is superior to the value reported for (+)-DTBZ (K_i = 0.97 nM (*33*)). In addition to imaging the basal ganglia region of the brain, this fluorinated DTBZ derivative, similar to its congener (+)-^{11}C-DTBZ (Fig. 1), could be a potential imaging agent to estimate the mass of β-cells related to the endocrine pancreas function in vivo. We report herein the initial evaluation of ^{18}F-FP-(+)-DTBZ in normal rats and evaluate the selectivity of pancreas uptake by blocking studies.

MATERIALS AND METHODS

General

Optically pure ^{18}F-FP-DTBZ was prepared by an ^{18}F-fluoride displacement of the corresponding mesylate, and the product was purified by high-performance liquid chromatography as described previously (*30,31*). The radiochemical purity of ^{18}F-FP-(+)-DTBZ was greater than 95%, and the specific activity was 55,500–74,000 GBq (1,500–2,000 Ci)/mmol at the end of synthesis. (+)-DTBZ and (+)9-O-desmethyl-α-dihydrotetrabenazine (used to prepare the mesylate precursor for ^{18}F-labeling) were kindly provided by the National Institute of Mental Health under the Chemical Synthesis and Drug Supply Program. Male Sprague–Dawley rats weighing 220–350 g were used for normal distribution and imaging studies.

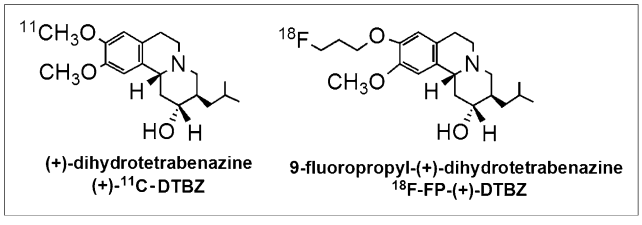

FIGURE 1. Potential PET agents for VMAT2.

Biodistribution Studies

Animals were anesthetized with isoflurane and then injected (intravenously via the femoral vein) with 0.2 mL of a saline solution containing ^{18}F-FP-(+)-DTBZ (active isomer) or ^{18}F-FP-(−)-DTBZ (inactive isomer) (0.37–0.74 MBq [10–20 μCi]). The rats (n = 3–4 for each time point) were then sacrificed under isoflurane anesthesia at indicated time points after injection. Organs of interest were removed and weighed, and the radioactivity was counted with an automatic γ-counter. The percentage dose per organ was calculated by comparing tissue counts with suitably diluted aliquots of the injected material. The total activity of the blood was calculated under the assumption that it was 7% of the total body weight. The percentage dose per gram of samples was calculated by comparing the sample counts with the count of the diluted initial dose. Different regions corresponding to striatum, hippocampus, cerebellum, and cortex were dissected from the brain and counted to obtain the regional distribution of the tracer.

To further prove that the accumulation of ^{18}F-FP-(+)-DTBZ in the pancreas was indeed due to the presence of VMAT2 binding sites, we pretreated the rats with (+)-DTBZ or FP-(+)-DTBZ (respectively, 3.8 and 3.5 mg/kg, intravenously), selective VMAT2 ligands, or FP-(−)-DTBZ (3.5 mg/kg, intravenously) at 5 min before tracer injection. Alternately, ^{18}F-FP-(+)-DTBZ was injected together with (+)-DTBZ (2.0 mg/kg). At 30 min after the tracer (or tracer with added carrier) injection, the rats were sacrificed; organs or tissues were removed and counted as described above. The significance in reduction of tracer binding in selected organ or tissues was determined by a Student t test.

Imaging Studies

The University of Pennsylvania has a small-animal PET scanner (*34*), the MOSAIC PET (Philips), used in this study to perform the PET imaging on control rats (220–350 g). Each animal was anesthetized initially using 3% isoflurane in 1.0 L/min oxygen, in an acrylic induction chamber. When fully anesthetized, the animal was placed on the scanner bed, with a nose cone used to maintain anesthesia at 1.5% isoflurane in 1.0 mL of oxygen per minute. Body temperature was maintained by placing a heating pad under the animal. A dose of 30–37 MBq (0.8–1 mCi) ^{18}F-FP-(+)-DTBZ (volume < 0.4 mL) was injected into the tail vein. A total of 24 dynamic scans (5 min/frame) were acquired over a course of 2 h. Images were reconstructed using a fully 3-dimensional iterative image reconstruction algorithm with system attenuation correction incorporated in the algorithm. Corrections were applied for scatter, randomness, and attenuation. Regions of interest (ROIs) were drawn, guided by a detailed rat atlas and micro-CT images. Visual analysis was performed using coronal, transverse, and sagittal reconstruction. ROIs were drawn over the pancreas as well as other organs or tissues. Mean counts per voxel in each region were calculated at various times.

RESULTS

The in vivo biodistribution study of ^{18}F-FP-(+)-DTBZ in rats clearly showed that the pancreas displayed the highest uptake among all organs or tissues in the body (5.5% dose/g

TABLE 1
In Vivo Biodistribution of ^{18}F-FP-(+)-DTBZ in Control Sprague–Dawley Rats

Region	Time after injection (min)			
	2	30	60	120
Blood	0.26 ± 0.03	0.23 ± 0.06	0.18 ± 0.02	0.12 ± 0.03
Heart	0.71 ± 0.07	0.41 ± 0.03	0.30 ± 0.10	0.22 ± 0.01
Muscle	0.14 ± 0.03	0.17 ± 0.02	0.13 ± 0.01	0.10 ± 0.01
Lung	0.94 ± 0.04	0.69 ± 0.03	0.54 ± 0.14	0.35 ± 0.03
Kidney	2.10 ± 0.17	1.06 ± 0.06	0.84 ± 0.09	0.55 ± 0.06
Pancreas	2.51 ± 0.22	5.50 ± 0.97	4.98 ± 0.24	2.76 ± 0.61
Spleen	1.46 ± 0.15	1.03 ± 0.18	0.83 ± 0.18	0.48 ± 0.04
Liver	3.53 ± 0.56	2.82 ± 0.24	2.47 ± 0.30	1.47 ± 0.13
Skin	0.23 ± 0.05	0.28 ± 0.01	0.23 ± 0.04	0.16 ± 0.02
Whole brain	0.71 ± 0.05	0.62 ± 0.08	0.42 ± 0.04	0.35 ± 0.02
Regional brain				
Cerebellum	0.63 ± 0.03	0.40 ± 0.04	0.28 ± 0.04	0.20 ± 0.01
Striatum	1.52 ± 0.20	2.25 ± 0.48	1.85 ± 0.26	1.42 ± 0.54
Hippocampus	0.68 ± 0.07	0.61 ± 0.12	0.36 ± 0.08	0.23 ± 0.03
Cortex	0.65 ± 0.02	0.44 ± 0.06	0.27 ± 0.07	0.20 ± 0.06
Remainder	0.70 ± 0.04	0.62 ± 0.08	0.44 ± 0.08	0.36 ± 0.08
Hypothalamus	1.23 ± 0.29	1.46 ± 0.40	1.21 ± 0.20	0.83 ± 0.10

Data are % dose/g, average of 3 rats ± SD. Regional brain distribution data are % dose/g ± SD.

TABLE 3
Biodistribution in Rats After Intravenous Injection of ^{18}F-FP-(−)-DTBZ

Region	Time after injection (min)	
	30	60
Blood	0.28 ± 0.02	0.16 ± 0.02
Pancreas	1.23 ± 0.02	0.57 ± 0.19
Striatum	0.16 ± 0.01	0.06 ± 0.02

Data are % dose/gram, average of 3 rats ± SD.

at 30 min after injection) (Table 1). The liver, an organ adjacent to the pancreas, showed a significant but lower uptake (2.8% dose/g) than the uptake observed in the pancreas. The washout of radioactivity from the pancreas was relatively slow, with 2.7% dose/g remaining at 2 h after injection. The high pancreas uptake observed with ^{18}F-FP-(+)-DTBZ is consistent with the reported value of 6.2% dose/g in rats for (+)-^{11}C-DTBZ (*26*). Other BCM ligands, such as sulfonylurea receptor ligand, glibenclamide, and fluorodithizone, a molecule exploiting the unique glucose-handling machinery of β-cells, displayed almost exclusive distribution in the liver with barely detectable amounts in the pancreas (*35*).

To confirm that pancreas uptake is specifically due to the VMAT2 signal, we performed blocking studies (via either pretreatment or coadministration with (+)-DTBZ or pretreatment with FP-(+)-DTBZ or FP-(−)-DTBZ) (*31*). In these experiments, the pancreas uptake was blocked by the competing dose of (+)-DTBZ (30% for pretreatment and 36% for coadministration). Pretreatment with FP-(+)-DTBZ (K_i = 0.11 nM) resulted in a greater blocking of the uptake in the pancreas (78%) (Table 2). As expected, the inactive isomer (K_i > 3,000 nM) showed very low inhibition of pancreas uptake (9%) (Table 3). In the same experiments, the striatal region (a brain region containing a high concentration of VMAT2 binding sites) showed a complete blocking of ^{18}F-FP-(+)-DTBZ uptake by the active isomer (Table 2), whereas the inactive isomer (Table 3), as expected, showed a very low inhibition of striatal uptake (Table 2). The lesser blocking of pancreas uptake by (+)-DTBZ (30%–36% blockage) was probably because in vivo kinetics of (+)-DTBZ may be different from those of FP-(+)-DTBZ. Higher pancreas blockage of ^{18}F-FP-(+)-DTBZ uptake by FP-(+)-DTBZ (78%) suggests matching kinetics between the cold and hot ligand binding to the same VMAT2 binding sites in the pancreas.

Small-animal PET was performed on Sprague–Dawley rats after an injection of ^{18}F-FP-(+)-DTBZ. The pancreas was clearly visualized in control rats (transverse, coronal, and sagittal views), with the pancreatic activity greater than the uptake activity of any other organ (Fig. 2). Quantitative

TABLE 2
Blocking Studies of Pancreatic Uptake of ^{18}F-FP-(+)-DTBZ at 30 Minutes After Tracer Injection in Rats

Region	Control	(+)-DTBZ pretreatment (3.8 mg/kg, intravenously, 5 min prior)	Control	(+)-DTBZ coinjection (2.0 mg/kg)	Control	FP-(+)-DTBZ pretreatment (3.5 mg/kg, intravenously, 5 min prior)	Control	FP-(−)-DTBZ pretreatment (3.5 mg/kg, intravenously, 5 min prior)
Blood	0.20 ± 0.01	0.32 ± 0.04	0.37 ± 0.01	0.44 ± 0.03	0.20 ± 0.02	0.26 ± 0.04	0.19 ± 0.02	0.21 ± 0.03
Pancreas	4.39 ± 0.64	3.10 ± 0.30*	5.95 ± 0.40	3.83 ± 0.25*	4.93 ± 0.49	1.11 ± 0.07*	4.97 ± 0.93	4.55 ± 0.64
Striatum	1.94 ± 0.03	0.27 ± 0.02	1.87 ± 0.14	0.28 ± 0.02	1.59 ± 0.23	0.24 ± 0.02	1.62 ± 0.03	1.47 ± 0.02

*$P < 0.05$.

Data are % dose/g, average of 3 rats ± SD. Significance in reduction of tracer binding in selected organ or tissues was determined by Student *t* test. Data showed 30% blockage in (+)-DTBZ pretreated group, 36% blockage in (+)-DTBZ coinjected group, and 78% blockage in FP-(+)-DTBZ pretreated group. Only 9% blockage was observed in FP-(−)-DTBZ pretreated group. Control rats were used for every blocking study; therefore, 4 sets of controls are included.

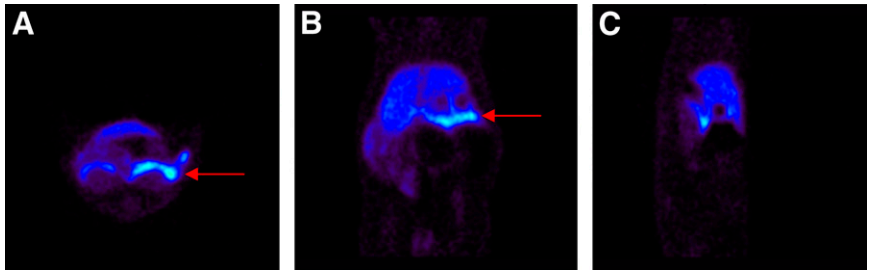

FIGURE 2. Representative in vivo PET images (data acquired at 30–35 min after tracer injection) of transverse, coronal, and sagittal views of abdominal planes of male Sprague–Dawley rat. ^{18}F-FP-(+)-DTBZ (33.3 MBq [0.9 mCi]) was injected into rat, after which animal was scanned for 2 h. Images were reconstructed and ROIs were defined. Red arrows indicate pancreas uptake.

measurements of radioligand uptake were obtained by placing ROIs in the liver, kidney, and pancreas (Fig. 3A). It appeared that ^{18}F-FP-(+)-DTBZ was removed from the blood by both liver and kidney. In the liver, ^{18}F-FP-(+)-DTBZ is excreted into the bile duct, showing a steady increase of accumulation of activity over the 2-h scanning period. Pancreatic ^{18}F-FP-(+)-DTBZ uptake increased from immediately after the intravenous injection to about 30–35 min after injection, followed by a slight washout. Because of lower accumulations of radioactivity in the muscle or kidney, these regions provide convenient reference regions. Our data obtained with ^{18}F-FP-(+)-DTBZ compare with the results reported previously with (+)-^{11}C-DTBZ and PET (*26*). The time–activity curves of ^{18}F-FP-(+)-DTBZ for pancreas, liver, kidney, and muscles obtained from PET correlated well with curves from the biodistribution data obtained by dissection and counting of the tissues (Fig. 3B). Thus, the imaging data were consistent with in vivo biodistribution results.

We have also performed preliminary binding studies with ^{18}F-FP-(+)-DTBZ using purified human islet homogenates. Specific VMAT2 binding signal was detected in the islet cell homogenates. The binding appeared to be saturable with a high binding affinity (data not shown). However, because of a limited supply of human β-cells, we have not been able to investigate this further.

DISCUSSION

We report the results of an initial study of ^{18}F-FP-(+)-DTBZ, a radiotracer targeting VMAT2 binding sites, as a potential imaging agent for BCM in the pancreas. Originally, the ^{18}F derivative was designed to image VMAT2 binding sites in the brain and is now in clinical trials to assess reductions of VMAT2 binding sites in patients with Parkinson's disease and dementia with Lewy bodies (*25*). Our interest in studying VMAT2 binding sites in the pancreas is based on recent reports suggesting that neurons in the pancreas share expression of a large number of genes and display functional similarity with neurons in the brain (*2,22*). That report indicated that a high density of VMAT2 is present in the β-cells of the pancreas with little or no VMAT2 in surrounding organs. Therefore, VMAT2 binding sites in the pancreas may serve as markers for functional β-cells. To test this hypothesis, we have studied the localization of ^{18}F-FP-(+)-DTBZ in the pancreas of normal rats. The specificity of ^{18}F-FP-(+)-DTBZ for VMAT2 binding in the pancreas was further confirmed by the in vivo competition with the specific VMAT2 ligand (+)-DTBZ as well as FP-(+)-DTBZ. Significantly, pretreatment of FP-(−)-DTBZ did not show any inhibition of pancreas uptake, suggesting ^{18}F-FP-(+)-DTBZ for VMAT2 binding in the pancreas is a highly selective and specific process.

The greater level of blocking by FP-(+)-DTBZ versus (+)-DTBZ suggests that the kinetics of the compounds are different. A significantly high nonspecific background distribution was also observed with (+)-^{11}C-DTBZ (*26*).

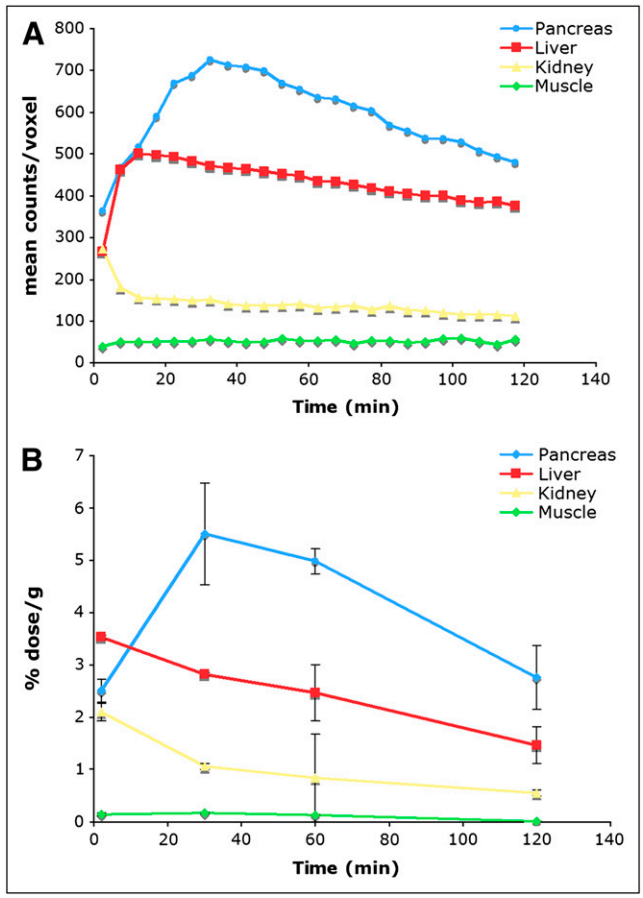

FIGURE 3. Quantitation of in vivo activity within pancreas, liver, kidney, and muscle ROIs during scan period is shown in time–activity curves. Consistently, observed time–activity curve via imaging (A) is very similar to results obtained with tissue dissection and counting method (B).

Whether this level of nonspecific distribution will impact the usefulness of the radioligand for PET studies of β-cell losses in disease remains to be seen. Increasing the signal with a higher specific VMAT2 binding in the pancreas will likely improve the potential for imaging BCM containing these VMAT2 binding sites.

While our work was in progress, an abstract describing ^{18}F-labeled 9-FCH$_2$-DTBZ for imaging BCM was presented at the 17th International Symposium on Radiopharmaceutical Sciences, April 30–May 4, 2007, in Aachen, Germany (*36*). The paper concluded that ^{18}F-labeled 9-FCH$_2$-DTBZ shows regional brain uptake and binding affinity similar to those shown by (+)-^{11}C-DTBZ, and it may be feasible to use ^{18}F-labeled 9-FCH$_2$-DTBZ as a PET tracer for measuring BCM. The report further confirmed our contention that ^{18}F-labeled DTBZ derivatives are excellent candidates for imaging BCM. Direct comparison studies will be needed to figure out which ligand shows better pancreas VMAT2 binding in vivo. Other imaging agents for imaging BCM have been reported, but none has demonstrated as promising properties as those demonstrated by VMAT2 imaging agents (*16,21*). The potential clinical application of various BCM imaging agents has been extensively reviewed (*1*).

CONCLUSION

^{18}F-FP-(+)-DTBZ has the potential to be a useful marker for BCM. High-quality PET images of the pancreas in normal rats can be obtained using this radiotracer. In conjunction with the findings on (+)-^{11}C-DTBZ, it seems clear that VMAT2 radioligand binding and PET imaging may be a useful way to evaluate BCM in the pancreas.

ACKNOWLEDGMENTS

We thank Dr. Henry Wagner for his helpful discussion and in selecting Figure 3 as the small-animal image of the year at the 2007 annual meeting of the Society of Nuclear Medicine. We are grateful to the Chemical Synthesis and Drug Supply Program of the National Institute of Mental Health for providing the samples of resolved (+)9-*O*-desmethyl-DTBZ-(−)-TBZ and other TBZ analogs used in this project. We also thank Dr. Paul Harris for his helpful discussion and Dr. Carita C. Huang for her editorial assistance.

REFERENCES

1. Souza F, Freeby M, Hultman K, et al. Current progress in non-invasive imaging of beta cell mass of the endocrine pancreas. *Curr Med Chem.* 2006;13:2761–2773.
2. Harris PE, Ferrara C, Barba P, Polito T, Freeby M, Maffei A. VMAT2 gene expression and function as it applies to imaging beta-cell mass. *J Mol Med.* 2008;86:5–16.
3. Murthy R, Harris P, Simpson N, et al. Whole body [^{11}C]-dihydrotetrabenazine imaging of baboons: biodistribution and human radiation dosimetry estimates. *Eur J Nucl Med Mol Imaging.* 2008;35:790–797.
4. Bertuzzi F, Marzorati S, Secchi A. Islet cell transplantation. *Curr Mol Med.* 2006;6:369–374.
5. Briones RM, Miranda JM, Mellado-Gil JM, et al. Differential analysis of donor characteristics for pancreas and islet transplantation. *Transplant Proc.* 2006;38:2579–2581.
6. Frank AM, Barker CF, Markmann JF. Comparison of whole organ pancreas and isolated islet transplantation for type 1 diabetes. *Adv Surg.* 2005;39:137–163.
7. Iwanaga Y, Matsumoto S, Okitsu T, et al. Living donor islet transplantation, the alternative approach to overcome the obstacles limiting transplant. *Ann N Y Acad Sci.* 2006;1079:335–339.
8. Pileggi A, Cobianchi L, Inverardi L, Ricordi C. Overcoming the challenges now limiting islet transplantation: a sequential, integrated approach. *Ann N Y Acad Sci.* 2006;1079:383–398.
9. Hampton T. Stem cells probed as diabetes treatment. *JAMA.* 2006;296:2785–2786.
10. Ren J, Jin P, Wang E, et al. Pancreatic islet cell therapy for type I diabetes: understanding the effects of glucose stimulation on islets in order to produce better islets for transplantation. *J Transl Med.* 2007;5:1.
11. Teague WJ, Rowan-Hull AM, Johnson PR. Pancreatic alpha-cell differentiation by mesenchyme-to-epithelial transition: implications for cell-based therapies in children. *J Pediatr Surg.* 2007;42:153–159.
12. Schmitz A, Shiue CY, Feng Q, et al. Synthesis and evaluation of fluorine-18 labeled glyburide analogs as beta-cell imaging agents. *Nucl Med Biol.* 2004;31:483–491.
13. Wangler B, Beck C, Shiue CY, et al. Synthesis and in vitro evaluation of (S)-2-([^{11}C]methoxy)-4-[3-methyl-1-(2-piperidine-1-yl-phenyl)-butyl-carbam oyl]-benzoic acid ([^{11}C]methoxy-repaglinide): a potential beta-cell imaging agent. *Bioorg Med Chem Lett.* 2004;14:5205–5209.
14. Wangler B, Schneider S, Thews O, et al. Synthesis and evaluation of (S)-2-(2-[^{18}F]fluoroethoxy)-4-([3-methyl-1-(2-piperidin-1-yl-phenyl)-butyl-carbamoyl]-methyl)-benzoic acid ([^{18}F]repaglinide): a promising radioligand for quantification of pancreatic beta-cell mass with positron emission tomography (PET). *Nucl Med Biol.* 2004;31:639–647.
15. Clark PB, Gage HD, Brown-Proctor C, et al. Neurofunctional imaging of the pancreas utilizing the cholinergic PET radioligand [^{18}F]4-fluorobenzyltrozamicol. *Eur J Nucl Med Mol Imaging.* 2004;31:258–260.
16. Hampe CS, Wallen AR, Schlosser M, Ziegler M, Sweet IR. Quantitative evaluation of a monoclonal antibody and its fragment as potential markers for pancreatic beta cell mass. *Exp Clin Endocrinol Diabetes.* 2005;113:381–387.
17. Anlauf M, Schafer MK, Schwark T, et al. Vesicular monoamine transporter 2 (VMAT2) expression in hematopoietic cells and in patients with systemic mastocytosis. *J Histochem Cytochem.* 2006;54:201–213.
18. Li H, Waites CL, Staal RG, et al. Sorting of vesicular monoamine transporter 2 to the regulated secretory pathway confers the somatodendritic exocytosis of monoamines. *Neuron.* 2005;48:619–633.
19. Markmann JF, Deng S, Desai NM, et al. The use of non-heart-beating donors for isolated pancreatic islet transplantation. *Transplantation.* 2003;75:1423–1429.
20. Schneider S, Feilen PJ, Schreckenberger M, et al. In vitro and in vivo evaluation of novel glibenclamide derivatives as imaging agents for the non-invasive assessment of the pancreatic islet cell mass in animals and humans. *Exp Clin Endocrinol Diabetes.* 2005;113:388–395.
21. Sweet IR, Cook DL, Lernmark A, Greenbaum CJ, Krohn KA. Non-invasive imaging of beta cell mass: a quantitative analysis. *Diabetes Technol Ther.* 2004;6:652–659.
22. Maffei A, Liu Z, Witkowski P, et al. Identification of tissue-restricted transcripts in human islets. *Endocrinology.* 2004;145:4513–4521.
23. Anlauf M, Eissele R, Schafer MK, et al. Expression of the two isoforms of the vesicular monoamine transporter (VMAT1 and VMAT2) in the endocrine pancreas and pancreatic endocrine tumors. *J Histochem Cytochem.* 2003;51:1027–1040.
24. Koeppe RA, Gilman S, Joshi A, et al. ^{11}C-DTBZ and ^{18}F-FDG PET measures in differentiating dementias. *J Nucl Med.* 2005;46:936–944.
25. Bohnen NI, Albin RL, Koeppe RA, et al. Positron emission tomography of monoaminergic vesicular binding in aging and Parkinson disease. *J Cereb Blood Flow Metab.* 2006;26:1198–1212.
26. Simpson NR, Souza F, Witkowski P, et al. Visualizing pancreatic beta-cell mass with [^{11}C]DTBZ. *Nucl Med Biol.* 2006;33:855–864.
27. Souza F, Simpson N, Raffo A, et al. Longitudinal noninvasive PET-based beta cell mass estimates in a spontaneous diabetes rat model. *J Clin Invest.* 2006;116:1506–1513.
28. Kim SJ, Doudet DJ, Studenov AR, et al. Quantitative micro positron emission tomography (PET) imaging for the in vivo determination of pancreatic islet graft survival. *Nat Med.* 2006;12:1423–1428.
29. Lu Y, Dang H, Middleton B, et al. Noninvasive imaging of islet grafts using positron-emission tomography. *Proc Natl Acad Sci USA.* 2006;103:11294–11299.

30. Goswami R, Ponde DE, Kung MP, Hou C, Kilbourn MR, Kung HF. Fluoroalkyl derivatives of dihydrotetrabenazine as positron emission tomography imaging agents targeting vesicular monoamine transporters. *Nucl Med Biol.* 2006;33:685–694.
31. Kung MP, Hou C, Goswami R, Ponde DE, Kilbourn MR, Kung HF. Characterization of optically resolved 9-fluoropropyl-dihydrotetrabenazine as a potential PET imaging agent targeting vesicular monoamine transporters. *Nucl Med Biol.* 2007;34:239–246.
32. Kilbourn MR, Hockley B, Lee L, et al. Pharmacokinetics of [^{18}F]fluoroalkyl derivatives of dihydrotetrabenazine in rat and monkey brain. *Nucl Med Biol.* 2007;34:233–237.
33. Kilbourn M, Lee L, Borght TV, Jewett D, Frey K. Binding of [alpha]-dihydrotetrabenazine to the vesicular monoamine transporter is stereospecific. *Eur J Pharmacol.* 1995;278:249–252.
34. Surti S, Karp JS, Perkins AE, et al. Imaging performance of A-PET: a small animal PET camera. *IEEE Trans Med Imaging.* 2005;24:844–852.
35. Sweet IR, Cook DL, Lernmark A, et al. Systematic screening of potential beta-cell imaging agents. *Biochem Biophys Res Commun.* 2004;314:976–983.
36. Hostetler ED, Patel S, Guenther I, et al. Characterization of a novel F-18 labelled radioligand for VMAT2. Paper presented at: 17th International Symposium on Radiopharmaceutical Sciences; April 30–May 4, 2007; Aachen, Germany.